Journal of Alloys and Compounds 660 (2016) 17–22

Contents lists available at ScienceDirect

Journal of Alloys and Compounds

journal homepage: http://www.elsevier.com/locate/jalcom

Reversible phase transformation gel-type ionic liquid compounds based on tungstovanadosilicates

Tianpei Huang [a], Zhirong Xie [a], Qingyin Wu [a, *], Wenfu Yan [b]

[a] *Department of Chemistry, Zhejiang University, Hangzhou 310027, PR China*
[b] *State Key Laboratory of Inorganic Synthesis and Preparative Chemistry, Jilin University, Changchun 130012, PR China*

A R T I C L E I N F O

Article history:
Received 24 June 2015
Received in revised form
12 October 2015
Accepted 30 October 2015
Available online 10 November 2015

Keywords:
Polyoxometalate
Ionic liquid
Phase transformation
Thermostability
Electrochemical property

A B S T R A C T

A series of new reversible phase transformation gel-type ionic liquid compounds, $[PyPS]_5SiW_{11}VO_{40}$, $[PyPS]_7SiW_9V_3O_{40}$, $[TEAPS]_5SiW_{11}VO_{40}$ and $[TEAPS]_7SiW_9V_3O_{40}$, have been synthesized from two organic ammoniums 1-(3-sulfonic group) propyl-pyridine (PyPS), 1-(3-sulfonic group) propyl-triethylammonium (TEAPS) and vanadium-substituted heteropoly acids $H_5SiW_{11}VO_{40}$ and $H_7SiW_9V_3O_{40}$. The products can undergo a phase transformation from viscous gel-state to liquid-state below 100 °C, and ionic conductivity up to 10^{-3} S cm^{-1} was observed at 110 °C for these gel-type POM-ILs. The relationship between the component elements of the products and their physicochemical property has been studied. Their thermostability was measured using thermogravimetric and differential thermal analysis (TG-DTA), and the result indicates that the less vanadium atoms there are inside the heteropoly anion, the more stable the POM-IL is at high temperature. Cyclic voltammetry is carried out to study their electrochemical properties in organic solution. The potential values of redox waves confirm that the oxidability of these gel-type POM-ILs can be controlled upon changing the number of vanadium atoms in the heteropolyanions.

1. Introduction

Heteropoly acids (HPAs) are a fascinating kind of inorganic metal-oxygen cluster compounds [1]. They play very important roles in catalysis, biology, electrochemistry and materials science as a consequence of their nanoscale size, simple composition, unique structures and tunable electronic and physical properties [2–5]. However, the demerits of HPAs, such as weak thermal stability, high sensitivity to atmospheric moisture and the difficulty in machining impeded their potential application [6]. For this reason, the design and synthesis of HPA derivatives have attracted researchers' attention. Recently, the massive range of applications has led to many deliberate assembly tactics for the design and synthesis of various HPA derivatives by exchanging the surface protons of the HPA core cluster by organic cations [7,8].

Ionic liquids (ILs) are fascinating molten salts that remain in the liquid state at low temperatures [9], and they are being increasingly studied owing to their various attractive properties [10–12]. It is interesting to note that some ILs can present in a gelled or semi-solid form, while still maintain the intrinsic properties of ILs, such as ionic conductivity, drug activity and solvent ability [13,14]. Such IL gels are easily shaped, and they can broaden the array of applications of ILs.

In the past decade, the design and synthesis of novel polyoxometalate-based ionic liquids (POM-ILs), which consisted of heteropoly anions and organic cations, have drawn a great deal of attention. They have emerged as the most potential compounds for their applications in catalysis, electrochemistry and nanotechnology [15,16]. In fact, it was found that the nature of cations has a remarkable influence on the structure and the characteristics of the heteropoly compounds [17]. One of the most important findings is that the POMs can be modified by certain organic cations through weak intermolecular interactions, such as H-bonding, π–π stacking and van der Waals interactions to prepare interesting gel-type hybrid materials [18–20]. Such POM-based gel-type materials are much easier to machine, and with some significant physical characters such as temperature-responsive behavior. They can be applied in some particular fields, for instance electrochemical capacitors and fuel cells [21].

Herein, we chose two sulfo-group grafted ammoniums cations (1-(3-sulfonic group) propyl-pyridine and 1-(3-sulfonic group) propyl-triethylammonium, abbreviated as PyPS and TEAPS, respectively) and two Keggin-type vanadium-substituted

---

* Corresponding author.
E-mail address: qywu@zju.edu.cn (Q. Wu).

http://dx.doi.org/10.1016/j.jallcom.2015.10.292

heteropoly acids ($H_5SiW_{11}VO_{40}$ and $H_7SiW_9V_3O_{40}$) to synthesize a series of gel-type POM-based ionic liquids, which exhibit reversible phase transformation from gel state to liquid state below 100 °C. Specifically, an investigation has been done on the effects of the elementary composition on the thermal stability and electrochemical properties of these gel-type ionic liquids. These new gel-type materials may be good candidates for the phase transformation electrolyte because of their advantages for both liquid electrolyte and solid state electrolyte. They will facilitate the application of POMs as functional materials in the area of electrochemistry.

2. Experimental section

2.1. Synthesis of the gel-type POM-ILs

1-(3-sulfonic group) propyl-pyridine (abbreviated as PyPS) and 1-(3-sulfonic group) propyl-triethylammonium (abbreviated as TEAPS) were synthesized according to the literature [8]. Pyridine (0.055 mol) and 1,3-propanesultone (0.05 mol) were dissolved in acetone (25 ml) and stirred at 50 °C for 4 h. A white precipitate (PyPS) was obtained and washed by acetone for three times, then dried under vacuum. Similarly, TEAPS can be prepared. $H_5SiW_{11}VO_{40}$ and $H_7SiW_9V_3O_{40}$ were synthesized by modification of the method according to the literature available [22,23].

The presynthesized PyPS and $H_5SiW_{11}VO_{40}$ ($H_7SiW_9V_3O_{40}$) were taken in 5:1 (7:1) mole ratio to give 1 mol of $[PyPS]_5SiW_{11}VO_{40}$ ($[PyPS]_7SiW_9V_3O_{40}$). Firstly, PyPS was added to an aqueous solution of $H_5SiW_{11}VO_{40}$ ($H_7SiW_9V_3O_{40}$), and then the mixture was stirred for 12 h at room temperature. Water was evaporated in a water bath at first and then removed in vacuum to give the products which exhibit gel-state. $[TEAPS]_5SiW_{11}VO_{40}$ and $[TEAPS]_7SiW_9V_3O_{40}$ were prepared accordingly. Scheme 1 shows the idealized reaction used to prepare the four POM-ILs. The obtained compounds are highly insoluble in tetrahydrofuran, acetone and ethyl acetate, and soluble in N, N-dimethylformamide and dimethyl sulfoxide.

Carbon, nitrogen, sulfur, silicon, tungsten and vanadium were analyzed by elemental analysis. Calculated for $[PyPS]_5SiW_{11}VO_{40}$: C: 12.80%; N: 1.87%; S: 4.27%; Si: 0.75%; W: 53.89%; V: 1.36%. Found: C: 11.68%; N: 1.73%; S: 4.32%; Si: 0.82%; W: 54.94%; V: 1.53%. Calculated for $[PyPS]_7SiW_9V_3O_{40}$: C: 17.29%; N: 2.52%; S: 5.77%; Si: 0.72%; W: 42.52%; V: 3.93%. Found: C: 15.85%; N: 2.36%; S: 5.02%; Si: 0.89%; W: 43.98%; V: 4.17%. Calculated for $[TEAPS]_5SiW_{11}VO_{40}$: C: 13.99%; N: 1.81%; S: 4.15%; Si: 0.73%; W: 52.35%; V: 1.32%. Found: C: 12.85%; N: 1.65%; S: 4.08%; Si: 0.86%; W: 53.78%; V: 1.44%. Calculated for $[TEAPS]_7SiW_9V_3O_{40}$: C: 18.70%; N: 2.42%; S: 5.55%; Si: 0.69%; W: 40.90%; V: 3.78%. Found: C: 17.68%; N: 2.66%; S: 5.42%; Si: 0.77%; W: 41.97%; V: 3.93%. The results indicate that the actual measurement values are consistent with the calculated values, which confirms the composition of four POM-ILs [24].

2.2. Chemicals and instrumentation

Inductively coupled plasma mass spectrometry (ICP-MS) analysis was determined on a Shimadzu V-1012 ICP-MS spectrometer. FTIR spectrum was recorded on a Nicolet Nexus 470 FT/IR spectrometer over the wave number range 400–4000 cm^{-1} using KBr pellets. X-ray powder diffraction pattern was obtained on a BRUKER D8 ADVANCE X-ray diffractometer using a Cu tube operated at 40 kV and 40 mA in the range of $2\theta = 4–40°$ at a rate of $0.02° \cdot s^{-1}$. The thermal stability of the sample was investigated using simultaneous thermogravimetry (TG) and differential thermal analysis (DTA) techniques from room temperature to 600 °C. Measurement was performed using a Shimadzu thermal analyzer in a Nitrogen stream, with a scanning rate of 10 °C min^{-1}. The conductivity measurement of the product was obtained using a DDS-11A conductivity meter. Cyclic voltammetry (CV) was performed with a CHI650C electrochemical workstation in N,N-dimethylformamide (DMF). All potentials were given with respect to a Ag/AgCl reference electrode. A glass electrode was used as the working electrode and platinum was used as the counter electrode in organic media. The concentration of substrate was 0.5 mM, and 0.1 M $NaClO_4$ was assigned as supporting electrolyte. All reagents were analysis grade.

3. Results and discussion

3.1. IR spectra

Fig. 1 shows IR spectra of the gel-type POM-ILs. Vibrations corresponding to heteropoly anions with Keggin structure appear at 700–1100 cm^{-1}. The vibrational frequencies fall in the sequence of

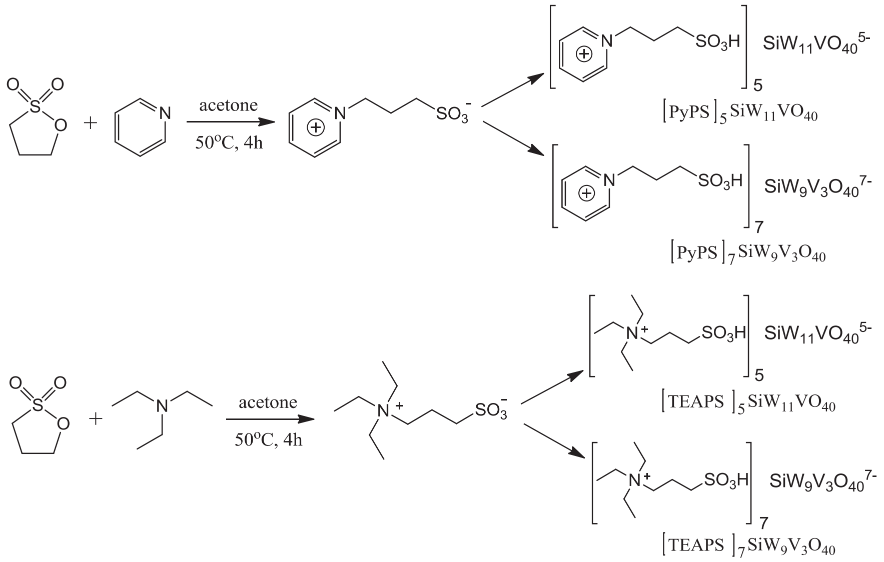

Scheme 1. Synthesis of the four POM-ILs.

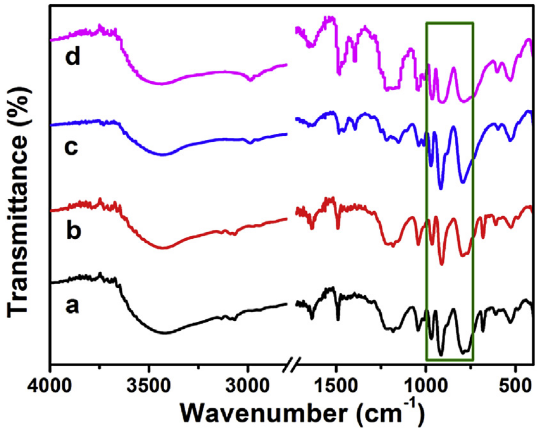

Fig. 1. IR spectra of the gel-type POM-ILs. (a) $[PyPS]_5SiW_{11}VO_{40}$; (b) $[PyPS]_7SiW_9V_3O_{40}$; (c) $[TEAPS]_5SiW_{11}VO_{40}$ and (d) $[TEAPS]_7SiW_9V_3O_{40}$.

ν_{as} (M–O_d) > ν_{as} (Si–O_a) > ν_{as} (M–O_b–M) > ν_{as} (M–O_c–M), (M = W, Mo, V), and O_a, O_b, O_c and O_d, each separately represent inner oxygen, corner-sharing oxygen, edge-sharing oxygen and terminal oxygen. There are characteristic bands of $[SiW_{11}VO_{40}]^{5-}$ in the IR spectrum of $[PyPS]_5SiW_{11}VO_{40}$ (curve a): 970 cm^{-1}, ν_{as} (M–O_d); 915 cm^{-1}, ν_{as} (Si–O_a); 880 cm^{-1}, ν_{as} (M–O_b–M); 793 cm^{-1}, ν_{as} (M–O_c–M). The similarities of the spectra of $[PyPS]_7SiW_9V_3O_{40}$ (curve b), $[TEAPS]_5SiW_{11}VO_{40}$ (curve c) and $[TEAPS]_7SiW_9V_3O_{40}$ (curve d) with $[PyPS]_5SiW_{11}VO_{40}$ strongly indicates that they have the same structure as $[SiM_{12}O_{40}]^{4-}$, showing that they still maintain Keggin structure though the introduction of vanadium atoms, which coincide with those reported in the literature for Keggin unit [25]. In comparison with the parent acids $H_5SiW_{11}VO_{40}$ and $H_7SiW_9V_3O_{40}$ according to the literature available [23,26], the ν_{as} (M–O_d) stretching vibration frequencies of these polyoxometalate compounds have red shifts after protons in the heteropoly acids were substituted by organic cations. The major reason may be that the introduced cations have stronger interactions to terminal oxygen atoms of the polyoxoanions, impairing the M–O_d bond, reducing the M–O_d bond force constant and leading to a decrease in the M–O_d vibration frequency [27]. The complete correlative assignments of the vibrational peaks of the POM-IL gels are listed in Table 1. Bands corresponding to both the organic cations and inorganic anions can be easily identified and confirm the formations of the hybrid molecular compounds. The bands at 1220–1236 cm^{-1}, which ascribed to S=O stretching vibrations, were detected to verify the existence of sulfonic groups in these two series of products [28]. Besides, PyPS cation shows other characteristic peaks at 1468–1485 cm^{-1} (pyridine ring), and 1144–1160 cm^{-1} (pyridine H–C–C and H–C–N bending). The results confirm the successful assembly and existence of the organic cation and Keggin unit in the compounds without depolymerization or degradation.

3.2. XRD patterns

The phase and structure of the obtained materials are further identified by using powder X-ray diffraction (XRD) in Fig. 2. The peaks in the XRD patterns of these POM-ILs are apparently different from that of the parent heteropoly acids. The broad diffraction peaks at the region of $2\theta = 15–38°$ of the products indicate smectic-state appearance of the samples, while their pure acids have high crystallinity [29]. The phase change of the hybrid molecular compounds was caused by the replacement of protons in HPA with PyPS and TEAPS cations [30].

In the small-angle region, the two monovanadium-substituted POM-ILs display different Bragg diffraction peaks from the trivanadium-substituted ones. $[PyPS]_5SiW_{11}VO_{40}$ presents visible peaks at $2\theta = 4.60°$ and 8.92°, which arises from the regular arrangement of the molecules in layers with a d-spacing of 1.92 nm [31]. Similarly, three Bragg diffraction peaks which appeared at 4.50°, 7.22°and 8.36° in the XRD pattern of $[TEAPS]_5SiW_{11}VO_{40}$ also indicate a layered structure with a d-spacing of 1.96 nm. According to the recent available paper, we can assume that such organized layer-type structure is formed via self-assembly of the heteropoly anions and organic cations through electrostatic interactions, hydrogen bondings, and Van der Waals forces [32]. However, $[PyPS]_7SiW_9V_3O_{40}$ shows only one peak at 8.25°, and $[TEAPS]_7SiW_9V_3O_{40}$ shows the peaks at 8.52° and 9.86°, which attributed to the characteristic peaks of Keggin structure at the region of $2\theta = 7–10°$ [33].

3.3. TG and DTA curves

Fig. 3 indicates TG and DTA curves of these gel-type POM-ILs. The initial minor weight loss below 150 °C is attributed to the loss of small amounts of absorbed water in the samples. The major weight loss between 300 and 400 °C is primarily due to the decomposition of both organic and inorganic parts of the compounds into their individual oxides. Generally, we take the temperature of the exothermic peak of DTA curve as the sign of their thermostability [34]. The decomposition temperature of $[PyPS]_5SiW_{11}VO_{40}$ (382 °C) is much higher than that of $[PyPS]_7SiW_9V_3O_{40}$ (344 °C). Similarly, $[TEAPS]_5SiW_{11}VO_{40}$ is thermally stable up to 351 °C, while the DTA curve of $[TEAPS]_7SiW_9V_3O_{40}$ shows that the decomposition occurs at 312 °C. The results demonstrate that the

Table 1
The complete correlative assignments of the vibrational peaks of the gel-type POM-ILs.

Wavenumber (cm^{-1})				Vibrations
$[PyPS]_5SiW_{11}VO_{40}$	$[PyPS]_7SiW_9V_3O_{40}$	$[TEAPS]_5SiW_{11}VO_{40}$	$[TEAPS]_7SiW_9V_3O_{40}$	
3423	3435	34,235	3445	O–H stretching
3070	3066	–	–	pyridine ring C–H stretching
2976	2976	2990	2990	alkyl C–H stretching
1635	1633	1635	1638	H–O–H bending
1489	1490	1482	1480	–CH_2 scissoring
–	–	1393	1390	–CH_2 twisting
1236	1230	1220	1220	S=O stretching
1144	1155	1149	1160	H–C–C & H–C–N bending
970	965	972	965	M–O_d stretching
915	911	917	912	Si–O_a stretching
884	–	881	–	M–O_b–M stretching
794	797	795	790	M–O_c–M stretching

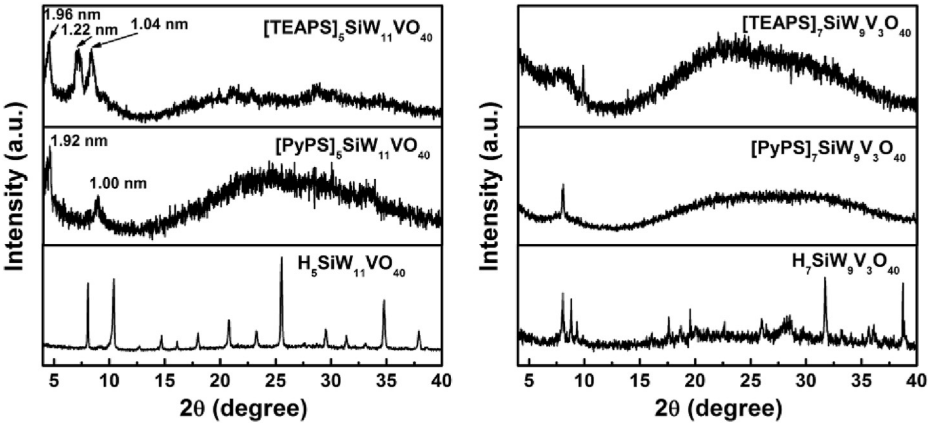

Fig. 2. XRD patterns of the gel-type POM-ILs and their corresponding parent acids.

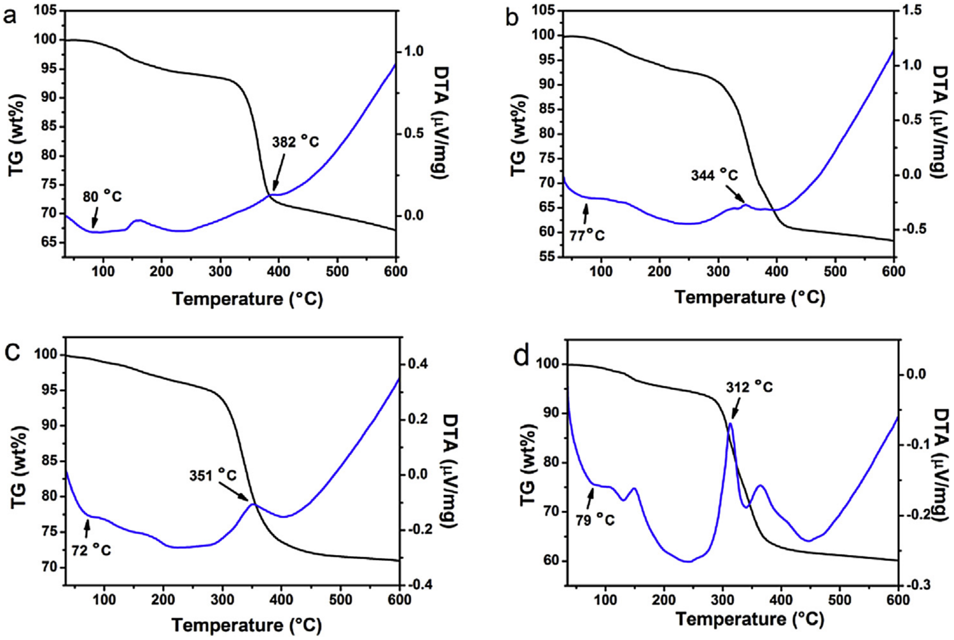

Fig. 3. TG and DTA curves of the POM-ILs, (a) $[PyPS]_5SiW_{11}VO_{40}$; (b) $[PyPS]_7SiW_9V_3O_{40}$; (c) $[TEAPS]_5SiW_{11}VO_{40}$ and (d) $[TEAPS]_7SiW_9V_3O_{40}$.

thermostability of the compounds will be enhanced when there are less vanadium atoms in POM anions.

On the other hand, the DTA curves of these gel-type POM-ILs show endothermic peaks located in the temperature range of 70–80 °C, which means that the POM-ILs can undergo a phase transformation from viscous gel-state to liquid-state [35]. The photographs of two different states of these compounds were shown in Fig. 4. This result confirms that they are temperature control-type POM-ILs.

3.4. Conductive property

Ionic conductivity of the POM-ILs is quite important for various applications. We have recorded the conductivity of these gel-type POM-ILs at different temperatures (Fig. 5). The conductivities of the products were measured for 6.47×10^{-3}, 8.28×10^{-3},

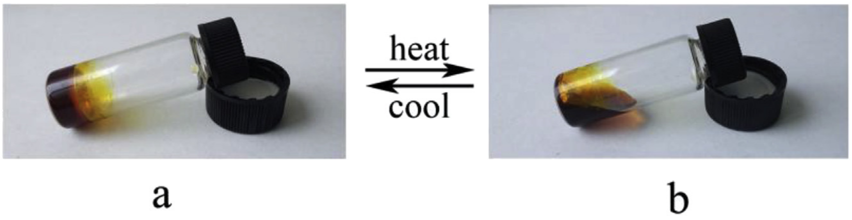

Fig. 4. Photographs of the two different states of the gel-type POM-ILs. (a) gel-state and (b) liquid-state.

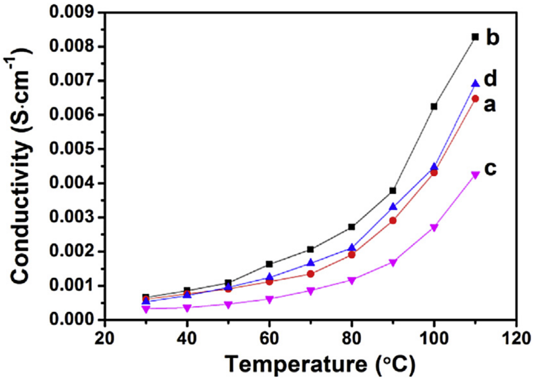

Fig. 5. Conductivity versus temperature plots of the gel-type POM-ILs, (a) $[PyPS]_5SiW_{11}VO_{40}$; (b) $[PyPS]_7SiW_9V_3O_{40}$; (c) $[TEAPS]_5SiW_{11}VO_{40}$ and (d) $[TEAPS]_7SiW_9V_3O_{40}$.

4.26×10^{-3} and 6.90×10^{-3} S cm^{-1} respectively at 110 °C. In the range of measured temperature, the ionic conductivity of these POM-ILs gradually increased with the temperature increasing. This can be explained as the decrease of the viscosity at elevated temperatures [36]. As shown in the conductivity–temperature plots in Fig. 5, the conductivities increase more rapidly after 70 °C, which is consistent with the observed phase transformation of the products begins at about 70 °C. All of these POM-ILs exhibit high conductivity more than 10^{-4} S cm^{-1} at room temperature and 10^{-3} S cm^{-1} at 110 °C. So these series of compounds can be regarded as a new kind of temperature-dependent POM-IL electrolytes.

3.5. Cyclic voltammetric behavior

A comparison of the cyclic voltammetric behavior of $[PyPS]_5SiW_{11}VO_{40}$, $[PyPS]_7SiW_9V_3O_{40}$, $[TEAPS]_5SiW_{11}VO_{40}$ and $[TEAPS]_7SiW_9V_3O_{40}$ in N,N-Dimethylformamide (DMF) containing 0.1 M $NaClO_4$ as the supporting electrolyte is shown in Fig. 6. They were evaluated at the different scan rates: 30, 60, 90, 120, 150 mV s^{-1}. The cathodic peak potentials of the samples slightly shifted towards negative values while the corresponding anodic peak potentials shifted to the positive values, the result indicates that a slow electron transfer exists [37,38]. In the potential range from −0.3–0.8 V, only a pair of reversible redox waves of $[PyPS]_5SiW_{11}VO_{40}$ was observed with formal potential at $E_f = 0.24$ V at a scan rate of 90 mV s^{-1}, where $E_f = (E_{pa} + E_{pc})/2$ (Fig. 6a). While $[TEAPS]_5SiW_{11}VO_{40}$ shows redox peaks with E_f values of 0.21 V. All of these waves correspond to reduction and oxidation of $SiW_{11}V^{V}O_{40}^{5-}$ and $SiW_{11}V^{IV}O_{40}^{6-}$ through a one-electron redox process, it can be described by the Eq. (1).

$$SiW_{11}V^{V}O_{40}^{5-} + e^- \rightarrow SiW_{11}V^{IV}O_{40}^{6-} \tag{1}$$

As for $[PyPS]_7SiW_9V_3O_{40}$ and $[TEAPS]_7SiW_9V_3O_{40}$, the successive redox peaks centered at 0.47 and 0.22 V, respectively, assigned formally to the V-center reductions. The electrochemical behaviors of the gel-type POM-ILs in DMF are summarized as shown in Eq. (2).

$$SiW_9V_3^{V}O_{40}^{7-} + 3e^- \rightarrow SiW_9V_3^{IV}O_{40}^{10-} \tag{2}$$

By comparison of these samples, the E_f of $[PyPS]_7SiW_9V_3O_{40}$ and $[TEAPS]_7SiW_9V_3O_{40}$ appears at a more positive potential than that of their corresponding monovanadium-substituted analogs. This result indicates that oxidability of trivanadium-substituted POM-ILs is greater than that of monovanadium-substituted POM-ILs, which would confirm that more vanadium atoms in the structure will bring about stronger oxidability at the same time. This leaves considerable flexibility in the choice of POMs for electrochemical purposes.

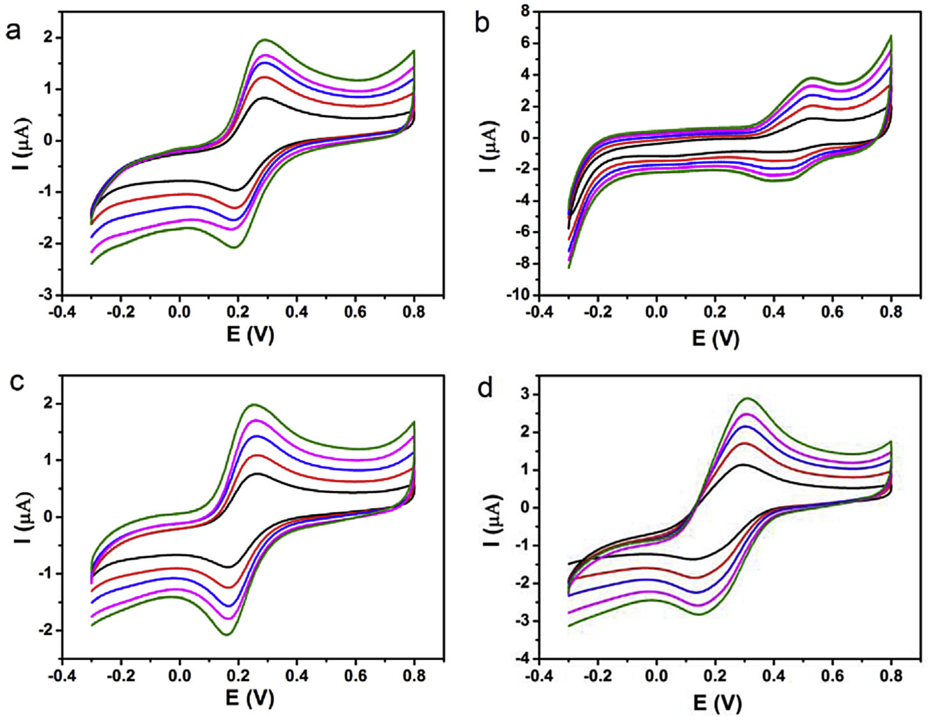

Fig. 6. Cyclic voltammetry of (a) $[PyPS]_5SiW_{11}VO_{40}$, (b) $[PyPS]_7SiW_9V_3O_{40}$, (c) $[TEAPS]_5SiW_{11}VO_{40}$ and (d) $[TEAPS]_7SiW_9V_3O_{40}$ in DMF at scan rates (inner to outer) of 30, 60, 90, 120 and 150 mV s^{-1}.

4. Conclusion

In this paper, we have reported some properties about a series of thermoregulated gel-type ionic liquids based on sulfo-group grafted ammonium and vanadium-substitutive POM anions, $[PyPS]_5SiW_{11}VO_{40}$, $[PyPS]_7SiW_9V_3O_{40}$, $[TEAPS]_5SiW_{11}VO_{40}$ and $[TEAPS]_7SiW_9V_3O_{40}$. They can undergo a reversible phase transformation from a quasi-solid-state gel phase to an isotropic sol phase and exhibit high ionic conductivity up to 10^{-3} S cm^{-1} at 110 °C. The results show that the thermostability and oxidability are closely related to the element composition of the POM-ILs. More vanadium atoms in the molecule will bring about lower thermostability and greater oxidability. These results contribute to provide some useful information for softening POM clusters in order to prepare POM-based functional materials, and promote the applications of such soft materials in the area of the electrochemistry.

Acknowledgments

This work was funded by the National Natural Science Foundation of China (21071124, 21173189), the Zhejiang Provincial Natural Science Foundation of China (LY14B030005) and the Foundation of State Key Laboratory of Inorganic Synthesis and Preparative Chemistry of Jilin University (2016-03).

References

[1] P.C. Yin, T. Li, R.S. Forgan, C. Lydon, X.B. Zuo, Z.N. Zheng, B. Lee, D.L. Long, L. Cronin, T.B. Liu, J. Am. Chem. Soc. 135 (2013) 13425–13432.
[2] H.Y. Zang, J.J. Chen, D.L. Long, L. Cronin, H. Miras, Adv. Mater. 25 (2013) 6245–6249.
[3] D. Ma, L.Y. Liang, W. Chen, H.M. Liu, Y.F. Song, Adv. Funct. Mater. 23 (2013) 6100–6105.
[4] C. Busche, L. Vilà-Nadal, J. Yan, H.N. Miras, D.L. Long, V.P. Georgiev, A. Asenov, R.H. Pedersen, N. Gadegaard, M.M. Mirza, D.J. Paul, J.M. Poblet, L. Cronin, Nature 515 (2014) 545–549.
[5] X. Tong, N.Q. Tian, W. Wu, W.M. Zhu, Q.Y. Wu, F.H. Cao, W.F. Yan, A.B. Yaroslavtsev, J. Phys. Chem. C 117 (2013) 3258–3263.
[6] P.E. Car, M. Guttentag, K.K. Baldridge, R. Alberto, G.R. Patzke, Green Chem. 14 (2012) 1680–1688.
[7] F. Yan, S. Yu, X. Zhang, L. Qiu, F. Chu, J. You, J. Lu, Chem. Mater. 21 (2009) 1480–1484.
[8] Y. Leng, J. Wang, D.R. Zhu, X.Q. Ren, H.Q. Ge, L. Shen, Angew. Chem. Int. Ed. 48 (2009) 168–171.
[9] T. Welton, Chem. Rev. 99 (1999) 2071–2084.
[10] S.K. Tang, G.A. Baker, H. Zhao, Chem. Soc. Rev. 41 (2012) 4030–4066.
[11] J.F. Ping, Y.X. Wang, Y.B. Ying, J. Wu, RSC Adv. 3 (2013) 19782–19784.
[12] L. Timperman, H. Galiano, D. Lemordant, M. Anouti, Electrochem. Commun. 13 (2011) 1112–1115.
[13] M. Armand, F. Endres, D.R. MacFarlane, H. Ohno, B. Scrosati, Nat. Mater. 8 (2009) 621–629.
[14] J. Le Bideau, L. Viau, A. Vioux, Chem. Soc. Rev. 40 (2011) 907–925.
[15] S. Herrmann, M. Kostrzewa, A. Wierschem, C. Streb, Angew. Chem. Int. Ed. 53 (2014) 1–5.
[16] Q.S. Yin, J.M. Tan, C. Besson, Y.V. Geletii, D.G. Musaev, A.E. Kuznetsov, Z. Luo, K.I. Hardcastle, C.L. Hill, Science 328 (2010) 342–345.
[17] Z.Y. Li, Q. Zhang, H.T. Liu, P. He, X.D. Xu, J.H. Li, J. Power Sources 158 (2006) 103–109.
[18] Y.L. Wang, W. Li, L.X. Wu, Langmuir 25 (2009) 13194–13200.
[19] P. He, B. Xu, H. Liu, S. He, F. Saleem, X. Wang, Sci. Rep. 3 (2013) 1833.
[20] Z.F. He, H.B. Wang, Y.L. Wang, Y. Wu, H.L. Li, L.H. Bi, L.X. Wu, Soft Matter 8 (2012) 3315–3321.
[21] J. Casamada Ribot, C. Guerrero-Sanchez, R. Hoogenboom, U.S. Schubert, Chem. Commun. 46 (2010) 6971–6973.
[22] P.J. Domaille, J. Am. Chem. Soc. 106 (1984) 7677–7678.
[23] N.Q. Tian, M.Y. Zhu, Q.Y. Wu, W.F. Yan, A.B. Yaroslavtsev, Mater. Lett. 115 (2014) 165–167.
[24] R.Y. Wang, D.Z. Jia, Y.L. Cao, Electrochimica Acta 72 (2012) 101–107.
[25] (a) A. Teze, G. Herve, Inorg. Synth. 27 (1990) 93;
(b) X. Tong, N.Q. Tian, W.M. Zhu, Q.Y. Wu, F.H. Cao, W.F. Yan, J. Alloys Compd. 544 (2012) 37–41;
(c) X. Tong, X.F. Wu, Q.Y. Wu, W.M. Zhu, F.H. Cao, W.F. Yan, Dalton Trans. 41 (2012) 9893–9896.
[26] T.P. Huang, N.Q. Tian, Q.Y. Wu, W.F. Yan, Soft Matter 11 (2015) 4481–4486.
[27] Z.K. Zhao, Y.T. Dai, T. Bao, R.Z. Li, G.R. Wang, J. Catal. 88 (2012) 44–53.
[28] X.X. Han, Y.F. He, C.T. Hung, L.L. Liu, S.J. Huang, S.B. Liu, Chem. Eng. Sci. 104 (2013) 64–72.
[29] X.K. Lin, W. Li, J. Zhang, H. Sun, Y. Yan, L.X. Wu, Langmuir 26 (2010) 13201–13209.
[30] W.L. Huang, W.S. Zhu, H.M. Li, H. Shi, G.P. Zhu, H. Liu, G.Y. Chen, Ind. Eng. Chem. Res. 49 (2010) 8998–9003.
[31] Y.X. Jiang, S.X. Liu, S.J. Li, J. Miao, J. Zhang, L.X. Wu, Chem. Commun. 47 (2011) 10287–10289.
[32] X.H. Yan, P.L. Zhu, J.B. Fei, J.B. Li, Adv. Mater. 22 (2010) 1283–1287.
[33] Y.P. Wang, B.B. Zhou, L.H. Zhang, J. Alloys Compd. 601 (2014) 126–129.
[34] X. Tong, W.M. Zhu, Q.Y. Wu, X.Y. Qian, Z. Liu, W.F. Yan, J. Gong, J. Alloys Compd. 509 (2011) 7768–7772.
[35] Y.Y. Li, T.P. Huang, Q.Y. Wu, H. Ding, W.F. Yan, A.B. Yaroslavtsev, Mater. Lett. 121 (2014) 159–161.
[36] K.F. Wang, F.F. Jian, R.R. Zhuang, Soft Matter 9 (2010) 32–43.
[37] A. Nicoara, A. Patrut, D. Margineanu, A. Müller, Electrochem. Commun. 5 (2003) 511–518.
[38] X.L. Wang, N. Li, A.X. Tian, J. Ying, T.J. Li, X.L. Lin, J. Luan, Y. Yang, Inorg. Chem. 53 (2014) 7118–7129.